Table V. Selected Bond Lengths (Å) and Angles (deg) for **2**

Tc(1)-Tc(2)	2.612 (2)		
Tc(1)-O(5)	1.967 (8)	Tc(2)-O(1)	1.988 (8)
Tc(1)-O(6)	2.023 (1)	Tc(2)-O(2)	2.041 (10)
Tc(1)-O(7)	2.039 (8)	Tc(2)-O(3)	2.040 (7)
Tc(1)-O(8)	1.991 (8)	Tc(2)-O(4)	1.966 (8)
Tc(1)-N(1)	1.937 (9)	Tc(2)-N(1)	1.954 (12)
Tc(1)-N(3)	1.935 (12)	Tc(2)-N(3)	1.936 (9)
N(1)-N(2)	1.311 (13)	N(3)-N(4)	1.297 (13)
O(5)-Tc(1)-O(6)	79.0 (4)	O(1)-Tc(2)-O(2)	78.2 (4)
O(5)-Tc(1)-O(7)	89.4 (3)	O(1)-Tc(2)-O(3)	92.5 (3)
O(5)-Tc(1)-O(8)	165.3 (4)	O(1)-Tc(2)-O(4)	167.5 (4)
O(5)-Tc(1)-N(1)	104.1 (4)	O(1)-Tc(2)-N(1)	86.0 (4)
O(5)-Tc(1)-N(3)	85.9 (4)	O(1)-Tc(2)-N(3)	103.1 (4)
O(6)-Tc(1)-O(7)	85.8 (4)	O(2)-Tc(2)-O(2)	86.1 (4)
O(6)-Tc(1)-O(8)	90.7 (4)	O(2)-Tc(2)-O(4)	92.6 (4)
O(6)-Tc(1)-N(1)	91.9 (4)	O(2)-Tc(2)-N(1)	164.0 (4)
O(6)-Tc(1)-N(3)	164.4 (4)	O(2)-Tc(2)-N(3)	91.0 (4)
O(7)-Tc(1)-O(8)	79.4 (3)	O(3)-Tc(2)-O(4)	78.3 (3)
O(7)-Tc(1)-N(1)	165.7 (4)	O(3)-Tc(2)-N(1)	92.1 (4)
O(7)-Tc(1)-N(3)	90.1 (4)	O(3)-Tc(2)-N(3)	163.2 (4)
O(8)-Tc(1)-N(1)	86.5 (4)	O(4)-Tc(2)-N(1)	102.7 (4)
O(8)-Tc(1)-N(3)	103.3 (4)	O(4)-Tc(2)-N(3)	85.3 (4)
N(1)-Tc(1)-N(3)	95.7 (5)	N(1)-Tc(2)-N(3)	95.1 (5)
Tc(1)-N(1)-N(2)	138.7 (10)	Tc(2)-N(1)-N(2)	137.0 (10)
Tc(1)-N(3)-N(4)	138.0 (10)	Tc(2)-N(3)-N(4)	137.0 (10)

with the hydrazido(2-) formalism rather than the isodiazene mode, which would require an N-N distance in the 1.15-1.20-Å range.

Another unusual feature of the structure of **2** is the presence of bridging hydrazido(2-) ligands,[43] a bonding mode that had been restricted to the cyclopentadienyl complexes $[Mo_2(C_5H_5)_2(NO)_2I_2(NNMe_2)]$[44] and $[Ti_2(C_5H_5)_2Cl_2(NNPh_2)_2]$.[45] Furthermore, in these latter complexes, the metal-bridging hydrazido nitrogen distances are unequivalent and the N-N distances lengthened to 1.39 Å. In contrast, the Tc-N distances for **2** are equivalent (1.925 (12)-1.954 (12) Å), while the average N-N distance of 1.31 (1) Å is consistent with the hydrazido(2-) formalism. Complex **2** is a unique example of symmetrically bridging η^1-hydrazido(2-) coordination.

The observation of bridging hydrazido ligands for **2** lends further support to the conclusion that the coordination chemistry of Tc-oxo precursors with organohydrazine ligands does not parallel that of Re-oxo and Mo-oxo species, where direct substitution of the terminal oxo group by a terminal hydrazido unit is the rule. Technetium-hydrazido chemistry is complicated by a tendency toward N-N bond cleavage and formation of Tc-nitrido and Tc-imido species[26] and by the presence of unusual bonding modes. The consequences of these results for bonding on the tracer level have yet to be evaluated.

We are currently investigating the magnetic and spectroscopic properties of **2** and of the related complexes $[Tc_2(NNRR')_2(cat)_4]^-$ (R = R' = CH_3, C_6H_5; R = CH_3, R' = C_6H_5; cat = $C_6Cl_4O_2^{2-}$, $C_6Br_4O_2^{2-}$, $C_6H_4O_2^{2-}$, $C_6H_2(t\text{-Bu})_2O_2^{2-}$).

Acknowledgment. This work was supported by a grant from Johnson Matthey.

Supplementary Material Available: For **1** and **2**, tables listing crystal data, details of the structure solution and refinement, atomic coordinates, bond distances and angles, anisotropic temperature factors, and calculated hydrogen atom positions (18 pages); listings of calculated and observed structure factors (57 pages). Ordering information is given on any current masthead page.

(43) Nicholson, T.; Zubieta, J. *Polyhedron* **1988**, *7*, 171 and references therein. Johnson, B. F. G.; Haymore, B. L.; Dilworth, J. R. In *Comprehensive Coordination Chemistry*; Wilkinson, G., Gillard, R. D., McCleverty, J. A., Eds.; Pergamon Press: Oxford, U.K., 1988; Chapter 13.3, pp 99-159. Sutton, D. *Chem. Soc. Rev.* **1975**, *4*, 443. Dilworth, J. R. *Coord. Chem. Rev.* **1976**, *21*, 29.

(44) Frisch, P. D.; Hunt, M. M.; Kita, W. G.; McCleverty, J. A.; Rose, A. E.; Seddon, D.; Swann, D.; Williams, J. *J. Chem. Soc., Dalton Trans.* **1979**, 1819.

(45) Hughes, D. L.; Latham, I. A.; Leigh, G. J. *J. Chem. Soc., Dalton Trans.* **1986**, 393.

(46) deLearie, L. A.; Haltiwanger, R. C.; Pierpont, C. G. *J. Am. Chem. Soc.* **1989**, *111*, 4324.

Contribution from the Departments of Chemistry, The Johns Hopkins University, Baltimore, Maryland 21218, and State University of New York (SUNY) at Albany, Albany, New York 12222

Fluoride as a Terminal and Bridging Ligand for Copper: Isolation and X-ray Crystallographic Characterization of Monomeric and Dimeric Complexes $[Cu^{II}(TMPA)F]_n^{n+}$ (n = 1 or 2; TMPA = Tris[(2-pyridyl)methyl]amine)

Richard R. Jacobson, Zoltán Tyeklár, Kenneth D. Karlin,* and Jon Zubieta

Received October 16, 1990

The copper(I) complex with tripodal tetradentate amine ligand TMPA, $[Cu^{I}(TMPA)CH_3CN]PF_6$ (**1**; TMPA = tris[(2-pyridyl)methyl]amine), reacts with dioxygen, resulting in breakdown of the hexafluorophosphate anion and providing two distinct fluoride Cu(II) complexes that have been crystallographically characterized. $[Cu^{II}(TMPA)F]_2(PF_6)_2$ (**2**) is a fluoride doubly bridged dimer (axial-equatorial), where each copper ion is pseudooctahedrally coordinated [$C_{36}H_{36}Cu_2F_{14}N_8P_2$, monoclinic $P2_1/n$; a = 11.649 (4), b = 12.942 (4), c = 14.654 (4) Å; β = 110.67 (2)°; Z = 4, V = 2067 (1) Å^3]. However, $[Cu^{II}(TMPA)F]PF_6 \cdot CH_2Cl_2$ (**3a**) contains a trigonal-bipyramidal (TBP) coordination environment, with axial fluoride and tertiary amine ligation [$C_{19}H_{20}Cl_2CuF_7N_4P$, orthorhombic $Pcab$; a = 11.869 (2), b = 15.891 (3), c = 26.116 (6) Å; Z = 8, V = 4926 (2) Å^3]. Complex **3a** readily loses its dichloromethane to give $[Cu^{II}(TMPA)PF_6 \cdot {}^1/_2H_2O$ (**3b**), which has solution properties (i.e. UV-vis, EPR) characteristic of TBP coordination. Compound **2** breaks down in solution to give the same monomeric structure as **3b**, and solution UV-vis and EPR studies indicate the **3b** structure can also be directly generated by addition of fluoride ion to $[Cu^{II}(TMPA)H_2O](ClO_4)$ (**4**).

In the last two decades, there has been a great deal of effort to synthesize low-molecular-weight complexes to model the function and/or spectroscopic features of copper-containing enzymes[1] and to explore relevant copper coordination chemistry in greater detail.[2] Fluoride ion binding to copper enzymes is of interest due to the use of F^- as a spectroscopic probe for proteins such as hemocyanin and tyrosinase and because of the known

* To whom correspondence should be addressed at the Department of Chemistry, The Johns Hopkins University, Charles & 34th Streets, Baltimore, MD 21218.

(1) *Copper Proteins and Copper Enzymes*; Lontie, R., Ed.; CRC Press: Boca Raton, FL, 1984; see also references cited therein.

(2) (a) *Copper Coordination Chemistry: Biochemical and Inorganic Perspectives*; Karlin, K. D., Zubieta, J., Eds.; Adenine: Guilderland, NY, 1983. (b) *Biological & Inorganic Copper Chemistry*; Karlin, K. D.; Zubieta, J. Eds.; Adenine Press: Guilderland, NY, 1986; Vols. 1 and 2. (c) Sorrell, T. N. *Tetrahedron* **1989**, *45*, 3-68.

0020-1669/91/1330-2035$02.50/0

deactivating effect of fluoride on metalloenzymes.[3,4] Furthermore, fluoride ligation in copper coordination complexes gives rise to compounds with unusual structural and magnetic properties.[5]

As a part of our efforts to prepare copper complexes with variable ligation and nonplanar coordination environments, we have been studying copper complexes of tripodal tetradentate ligands.[6] The investigation of the reaction of $[Cu^{I}(TMPA)CH_3CN]PF_6$ (**1**) (TMPA = tris[(2-pyridyl)methyl]amine) with

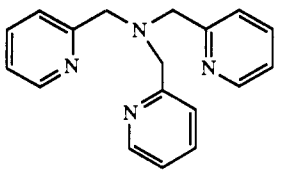

TMPA

dioxygen at −80 °C led to the disovery of the first structurally characterized copper dioxygen complex.[6b,c] Here we report that oxygenation of **1** at *ambient temperatures* results in the formation of mono- and dinuclear fluorocopper(II) complexes, which have been structurally characterized.

Experimental Section

Materials and Methods. The compound $[Cu^{I}(TMPA)CH_3CN]PF_6$ (**1**) was prepared by a literature method.[6b,c]

Reagents and solvents used were of commercially available reagent quality unless otherwise stated. Diethyl ether was purified by passing it through activated alumina. Preparations and handling of air-sensitive materials were carried out under an argon atmosphere by using standard Schlenk techniques. Deoxygenation of solvents and solutions was effected by bubbling (20 min) of Ar directly through the solutions. Solid samples were stored and transferred and samples for IR and NMR spectra were prepared in a Vacuum/Atmospheres drybox filled with argon. Elemental analyses were performed by Galbraith Laboratories, Inc., Knoxville, TN, and/or MicAnal, Tuscon, AZ.

Infrared spectra were recorded as Nujol mulls on either a Perkin-Elmer 283 or 710B instrument and calibrated with a polystyrene film. Electrical conductivity measurements were carried out in acetonitrile with a Barnstead Model PM-70CB conductivity bridge and a YSI Model 3403 conductivity cell. The cell constant was determined by using a standard aqueous KCl solution. Room-temperature magnetic moments were determined by using a Johnson Matthey magnetic susceptibility balance, and the instrument was calibrated by using $Hg[Co(SCN)_4]$. Electron paramagnetic resonance (EPR) spectra were obtained in frozen solutions at 77 K with 4-mm-o.d. quartz tubes in a Varian Model E-4 spectrometer operating at the X-band frequency. The field was calibrated with a powder sample of diphenylpicrylhydrazyl (DPPH, $g = 2.0037$). The solvent used was CH_2Cl_2–toluene (1:1, v:v), and concentrations of copper complexes were approximately 10^{-3} M.

$[Cu^{II}(TMPA)F]_2(PF_6)_2$ (2) and $[Cu^{II}(TMPA)F]PF_6 \cdot {}^1/_2H_2O$ (3b). The following synthetic procedure is a general method for preparing the title compounds, which are isolated from the same reaction mixture.

A 100-mL Schlenk flask was charged with 0.500 g (0.926 mmol) of $[Cu^{I}(TMPA)CH_3CN]PF_6$ (**1**) and a magnetic stirring bar. Acetonitrile (35 mL) was bubbled with argon for 20 min and added to the Cu(I) complex, and the resulting orange solution was stirred for 10 min. The flask was then evacuated and purged with O_2, causing an immediate change in color to violet and then cloudy green. The solution was stirred under an oxygen atmosphere for 48 h and eventually became light blue in color. It was filtered, and excess diethyl ether (250 mL) was added to give a crude precipitate, which was stored at 8 °C (refrigerator) for 24 h. After decantation, the precipitate was recrystallized by dissolving it in CH_2Cl_2 (30 mL) and layering the solution with ether (100 mL). After 24–48 h at 8 °C, a layer of green oil is deposited, which generally was found to contain a mixture of light blue (turquoise) and dark blue crystals. Occasionally, only one type of crystal was observed. The solid material was separated from the oil and recrystallized a second time from CH_2Cl_2–Et_2O. When a mixture of light and dark blue crystals was obtained, the crystals were manually separated according to color and recrystallized again. The green oil may also be redissolved in CH_2Cl_2 and layered with diethyl ether in an attempt to obtain additional crystalline material.

The dark blue crystals, formulated as $[Cu^{II}(TMPA)F]_2(PF_6)_2$ (**2**), were obtained in yields ranging from 0 to ca. 50% (based on Cu). Anal. Calcd for $C_{36}H_{36}Cu_2F_{14}N_8P_2$: C, 41.75; H, 3.50; N, 10.82; F, 25.68. Found: C, 41.94; H, 3.47; N, 10.93; F, 25.35. IR (Nujol; cm^{-1}): 840 (vs, br, PF_6^-), 490 (s, Cu–F).[7] UV-vis (CH_3CN): λ_{max} (ϵ, M^{-1} cm^{-1}) = 255 (10800), 714 (sh, 104), 882 (201) nm. Molar conductivity (CH_3CN): 147 Ω^{-1} cm^2 mol^{-1}. EPR (CH_2Cl_2–toluene): $g_{\parallel} = 1.955$, $A_{\parallel} = 81 \times 10^{-4}$ cm^{-1}, $g_{\perp} = 2.223$, $A_{\perp} = 99 \times 10^{-4}$ cm^{-1}. Magnetism (solid state, room temperature): $\mu_{eff} = 1.95 \pm 0.05$ μ_B/Cu.

The freshly isolated light blue crystalline material has been formulated as $[Cu^{II}(TMPA)F]PF_6 \cdot CH_2Cl_2$ (**3a**) on the basis of the results of an X-ray crystal structure determination. However, if this material is allowed to air dry, it quickly loses CH_2Cl_2, becoming a non/crystalline blue powder formulated as $[Cu^{II}(TMPA)F]PF_6 \cdot {}^1/_2H_2O$ (**3b**). The yields are generally observed to be low, ranging from 0 to 25% (based on Cu). Anal. Calcd for $C_{18}H_{19}CuF_7N_4O_{0.5}P$ ($[Cu^{II}(TMPA)F]PF_6 \cdot {}^1/_2H_2O$ (**3b**)): C, 41.03; H, 3.63; N, 10.63; F, 25.24. Found; C, 41.07; H, 3.76; N, 10.63; F, 24.98. IR (Nujol; cm^{-1}): 3645 (s, H_2O), 3625 (m), 3510 (m), 3340 (s), ca. 3220 (s, br, H_2O), 1655 (m, H_2O), 835 (vs, br, PF_6^-), 485 (s, Cu–F).[7] The solution properties of this compound are essentially identical with those of **2**. Molar conductivity (CH_3CN): 149 Ω^{-1} cm^2 mol^{-1}. UV-vis (CH_3CN): λ_{max} (ϵ, M^{-1} cm^{-1}) = 254 (10600), 715 (sh, 99), 881 (192) nm. EPR (CH_2Cl_2–toluene, 77 K): $g_{\parallel} = 1.954$, $A_{\parallel} = 80 \times 10^{-4}$ cm^{-1}, $g_{\perp} = 2.224$, $A_{\perp} = 94 \times 10^{-4}$ cm^{-1}.

Removal of Water from $[Cu^{II}(TMPA)F]PF_6 \cdot {}^1/_2H_2O$ (3b). A small quantity (ca. 100 mg) of $[Cu^{II}(TMPA)F]PF_6 \cdot {}^1/_2H_2O$ (**3b**) was added to a vial and placed within an Abderhalden drying apparatus (Ace 9632-10). The sample was placed under vacuum and heated to 85 °C for 38 h. After heating, the sample was removed from the apparatus under argon and submitted for elemental analysis and IR spectroscopy. The results indicated loss of water from **3b** to give a compound formulated as $[Cu^{II}(TMPA)F]PF_6$. Thermogravimetric analysis also confirmed the quantitative loss of water from **3b**. Anal. Calcd for $C_{18}H_{18}CuF_7N_4P$: C, 41.75; H, 3.50; N, 10.82; F, 25.24. Found: C, 41.50; H, 3.41; N, 10.31. IR (Nujol; cm^{-1}): 835 (vs, br, PF_6^-).

$[Cu^{II}(TMPA)H_2O](ClO_4)_2$ (4). TMPA (1.00 g, 3.45 mmol) and $Cu(ClO_4)_2 \cdot 6H_2O$ (1.28 g, 3.45 mmol) were dissolved in 50 mL of wet acetone and stirred for 45 min as a dark blue solution developed. Layering the solution with diethyl ether (75 mL) and storage at 8 °C for 24 h resulted in the formation of a light blue crystalline solid. Recrystallization from acetone/ether gave 1.45 g (73%) of **4** as blue crystals. Anal. Calcd for $C_{18}H_{20}Cl_2CuN_4O_9$: C, 37.87; H, 3.53; N, 9.81. Found: C, 38.16; H, 3.60; N, 9.73. IR (Nujol: cm^{-1}): ca. 3230 (vs, br H_2O), 2005 (w, ClO_4^- overtone), 1650 (m, H_2O), 1070 (vs, br, ClO_4^-). UV-vis (H_2O–MeOH–EtOH): λ_{max} (ϵ, M^{-1} cm^{-1})) = 870 (213) nm. EPR (H_2O–MeOH–EtOH): $g_{\parallel} = 2.004$, $A_{\parallel} = 59 \times 10^{-4}$ cm^{-1}, $g_{\perp} = 2.198$, $A_{\perp} = 100 \times 10^{-4}$ cm^{-1}.

Reaction of $[Cu^{II}(TMPA)H_2O](ClO_4)_2$ (4) with Tetrabutylammonium Fluoride Trihydrate. An UV–Vis and EPR Spectroscopy Study. Complex $[Cu^{II}(TMPA)H_2O](ClO_4)_2$ (**4**) (0.2282 g, 0.40 mmol) was weighed in a 10-mL volumetric flask and dissolved in methanol (solution A). Tetrabutylammonium fluoride trihydrate (0.2520 g, 0.80 mmol) was dissolved in ethanol in a 10-mL volumetric flask (solution B). Solution A (2.0 mL) was pipetted into a 10-mL volumetric flask and 1.0 and 5.0 mL of solution B (which correspond to 1.0 and 5.0 equiv of fluoride per copper, respectively) were added and the flask was filled to the mark with

(3) (a) Solomon, E. I. In *Metal Ions in Biology*; Spiro, T. H., Ed.; Wiley-Interscience: New York, 1981; Vol. 3, pp 41–108. (b) Himmelwright, R. S.; Eickman, N. C.; LuBien, C. D.; Solomon, E. I. *J. Am. Chem. Soc.* **1980**, *102*, 5378. (c) Himmelwright, R. S.; Eickman, N. C.; LuBien, C. D.; Lerch, K.; Solomon, E. I. *J. Am. Chem. Soc.* **1980**, *102*, 7339. (d) Winkler, M. E.; Lerch, K.; Solomon, E. I. *J. Am. Chem. Soc.* **1981**, *103*, 7001.

(4) Dooley, D. M. *Life Chem. Rep.* **1987**, *5*, 91–154 and references cited therein.

(5) (a) Reedijk, J. *Comments Inorg. Chem.* **1982**, *1*, 379–389. (b) Hayes, P. C.; Jones, G. *J. Chem. Soc., Chem. Commun.* **1980**, 844. (c) van Rijn, J.; Reedijk, J.; Dartmann, M.; Krebs, B. *J. Chem. Soc., Dalton Trans.* **1987**, 2579–2593. (d) Reedijk, J.; ten Hoedt, R. W. M. *Recl.: J. R. Neth. Chem. Soc.* **1982**, 49–57 and references cited therein. (e) Emsley, J.; Arif, M.; Bates, P. A.; Hursthouse, M. B. *J. Chem. Soc., Dalton Trans.* **1987**, 2397–2399. (f) Oosterling, A. J.; De Graaff, R. A. G.; Haasnoot, J. G.; Keij, F. S.; Reedijk, J.; Pedersen, E. *Inorg. Chim. Acta* **1989**, *163*, 53–58.

(6) (a) Zubieta, J.; Karlin, K. D.; Hayes, J. C. In ref 2a, pp 97–108. (b) Jacobson, R. R.; Tyeklár, Z.; Farooq, A.; Karlin, K. D.; Liu, S.; Zubieta, J. *J. Am. Chem. Soc.* **1988**, *110*, 3690–3692. (c) Jacobson, R. R. Ph.D. Dissertation, State University of New York at Albany, 1989. (d) Karlin, K. D.; Hayes, J. C.; Juen, S.; Hutchinson, J. P.; Zubieta, J. *Inorg. Chem.* **1982**, *21*, 4106–4108.

(7) The ν(Cu–F) stretching frequencies were assigned by comparison of the IR spectra of **2** and **3b** with those of $[Cu^{II}(TMPA)Cl]PF_6$ and $[Cu^{II}(TMPA)Br]PF_6$.[6c]

Table I. Crystallographic Data for Complexes $[Cu^{II}(TMPA)F]_2(PF_6)_2$ (**2**) and $[Cu^{II}(TMPA)F]PF_6 \cdot CH_2Cl_2$ (**3a**)

	2	**3a**
chem formula	$C_{36}H_{36}Cu_2F_{14}N_8P_2$	$C_{19}H_{20}Cl_2CuF_7N_4P$
fw	1035.76	602.81
space group	$P2_1/n$	$Pcab$
a, Å	11.649 (4)	11.869 (2)
b, Å	12.942 (4)	15.891 (3)
c, Å	14.654 (4)	26.116 (6)
α, deg	90.00	90.00
β, deg	110.67 (2)	90.00
γ, deg	90.00	90.00
V, Å^3	2067 (1)	4926 (2)
Z	4	8
ρ_{calcd}, g cm^{-3}	1.664	1.628
temp, K	294	294
λ, Å	0.71073	0.71073
μ, cm^{-1}	11.97	12.35
R^a	0.0518	0.0665
R_w^b	0.0585	0.0656

$^a R = \sum[|F_o| - |F_c|/\sum|F_o|]$. $^b R_w = [\sum w(|F_o| - |F_c|)^2/\sum w|F_c|^2]^{1/2}$. $w = 1/\delta^2(F_o) + g^*(F_o)^2$; $g = 0.005$.

Table II. Atom Coordinates (×10^4) and Temperature Factors (Å^2 × 10^3) for Compound $[Cu^{II}(TMPA)F]_2(PF_6)_2 \cdot CH_2Cl_2$ (**2**)

atom	x	y	z	$U_{equiv/iso}$[a]
Cu	1405 (1)	420 (1)	4 (1)	46 (1)*
P	2993 (2)	590 (1)	5842 (2)	75 (1)*
F1	1269 (4)	-805 (3)	624 (2)	67 (2)*
F2	3174 (17)	1111 (15)	6860 (14)	159 (9)*
F3	2675 (11)	-446 (5)	6250 (6)	115 (4)*
F4	2755 (13)	68 (13)	4827 (10)	119 (5)*
F5	3412 (11)	1587 (5)	5493 (7)	185 (7)*
F6	1650 (8)	949 (9)	5497 (6)	158 (5)*
F7	4361 (10)	172 (12)	6371 (11)	169 (7)*
N1	1288 (4)	1771 (3)	-740 (3)	47 (2)*
N2	1639 (4)	1348 (3)	1134 (3)	49 (2)*
N3	924 (4)	-171 (4)	-1325 (3)	49 (2)*
N4	3483 (4)	714 (4)	324 (4)	54 (2)*
C21	2078 (6)	1082 (4)	59 (4)	59 (2)
C22	2334 (6)	1798 (5)	2804 (5)	66 (2)
C23	2112 (6)	2808 (6)	2550 (5)	77 (2)
C24	1687 (6)	3114 (5)	1592 (5)	67 (2)
C25	1448 (5)	2360 (4)	901 (4)	54 (2)
C26	920 (6)	2574 (5)	-171 (4)	63 (2)
C31	1039 (5)	-1163 (5)	-1538 (4)	58 (2)
C32	710 (6)	-1484 (6)	-2486 (5)	74 (2)
C33	256 (7)	-773 (6)	-3201 (6)	84 (2)
C34	116 (7)	220 (5)	-3008 (5)	74 (2)
C35	474 (5)	522 (4)	-2036 (4)	52 (2)
C36	326 (6)	1580 (4)	-1715 (4)	60 (2)
C41	4470 (6)	330 (5)	1014 (5)	66 (2)
C42	5577 (7)	839 (5)	1367 (5)	73 (2)
C43	5658 (7)	1772 (6)	1028 (5)	81 (2)
C44	4648 (6)	2213 (5)	312 (4)	65 (2)
C45	3566 (5)	1633 (5)	-24 (4)	51 (1)
C46	2474 (5)	2013 (5)	-843 (4)	59 (2)

[a] Equivalent isotropic U is defined as one-third of the trace of the orthogonalized U_{ij} tensor and is marked with an asterisk. The anisotropic displacement exponent takes the form $-2\pi^2(h^2a^{*2}U_{11} + ... + 2hka^*b^*U_{12})$.

ethanol. The resulting 4:1 ethanol–methanol mixture was transferred into either a UV–vis cuvette (1-cm path length) or EPR tube for spectral analysis.

Crystallographic Data Collection and Structure Refinement. Crystals of compounds **2** and **3a** were grown by slow diffusion of diethyl ether into dichloromethane solutions of the complexes at 8 °C. Crystals suitable for X-ray structural analysis were mounted on a Nicolet R3m diffractometer with glass fibers; the crystal of **3a** was coated with epoxy to prevent loss of CH_2Cl_2 solvent. Diffraction intensities were measured by employing the θ–2θ scan technique; standard reflections measured during data collection showed only statistical variations in intensity. The positional parameters of the copper atom were determined by the Patterson method while the remaining non-hydrogen atoms were located on difference Fourier maps. Hydrogen atoms were calculated and fixed at 0.96 Å from carbon. Anisotropic refinement was carried out on Cu, N, P, and F atoms of **2** and **3a** (the PF_6^- anion in **3a** was observed to be disordered). The final R factors appear in Table I along with a summary of unit cell parameters, data collection parameters, and refinement results. Positional parameters are listed in Tables II and III, while selected bond distances and angles appear in Table IV.

Table III. Atom Coordinates (×10^4) and Temperature Factors (Å^2 × 10^3) for Compound $[Cu^{II}(TMPA)F]PF_6 \cdot CH_2Cl_2$ (**3a**)

atom	x	y	z	U_{equiv}[a]
Cu	796 (1)	1501 (1)	1140 (1)	53 (1)
F	-631 (4)	1962 (3)	1081 (2)	53 (2)
N1	2386 (7)	994 (5)	1205 (3)	50 (3)
N2	356 (7)	354 (5)	1406 (3)	52 (3)
N3	1485 (6)	2333 (5)	1645 (3)	51 (3)
N4	1324 (8)	1729 (5)	450 (4)	71 (4)
C21	-655 (10)	105 (7)	1612 (4)	63 (3)
C22	-831 (11)	-705 (8)	1775 (5)	76 (3)
C23	28 (11)	-1293 (9)	1717 (5)	87 (4)
C24	1033 (9)	-1065 (7)	1517 (4)	60 (3)
C25	1227 (9)	-240 (6)	1357 (4)	54 (3)
C26	2230 (9)	75 (6)	1138 (4)	57 (3)
C31	1084 (9)	3108 (7)	1768 (4)	59 (3)
C32	1658 (9)	3634 (7)	2120 (4)	59 (3)
C33	2635 (10)	3339 (7)	2339 (5)	73 (3)
C34	3031 (10)	2549 (7)	2221 (4)	60 (3)
C35	2482 (8)	2040 (6)	1872 (4)	46 (2)
C36	2771 (10)	1176 (7)	1715 (4)	63 (3)
C41	660 (12)	1999 (8)	10 (5)	78 (4)
C42	1154 (13)	2102 (9)	-460 (6)	99 (5)
C43	2300 (11)	1914 (8)	-540 (6)	80 (4)
C44	2907 (11)	1699 (7)	-179 (5)	76 (4)
C45	2495 (10)	1580 (7)	342 (4)	65 (3)
C46	3096 (10)	1380 (8)	805 (4)	68 (3)
P	-4566 (3)	-1027 (2)	1727 (1)	69 (1)
F1	-5700 (11)	-1468 (8)	1573 (5)	141 (4)
F2	-5372 (11)	-354 (8)	2027 (5)	105 (4)
F3	-3506 (15)	-535 (10)	1597 (7)	173 (6)
F4	-4067 (19)	-1821 (13)	1400 (9)	109 (7)
F5	-4760 (12)	-1585 (9)	2225 (5)	154 (5)
F6	-3698 (14)	-669 (10)	2128 (7)	157 (5)
F7	-5176 (20)	-152 (14)	1661 (9)	86 (7)
F8	-4588	-303	1294	104 (7)
F9	-3652 (15)	-1801 (10)	1701 (7)	113 (5)
F10	-4820 (24)	-1013 (18)	1101 (11)	246 (1)
Cl1	3695 (3)	4702 (2)	256 (1)	87 (1)
Cl2	1370 (3)	4190 (3)	198 (2)	108 (2)
C1	2582 (12)	4283 (8)	534 (5)	97 (6)

[a] Equivalent isotropic U is defined as one-third of the trace of the orthogonalized U_{ij} tensor. The anisotropic displacement exponent takes the form $-2\pi^2(h^2a^{*2}U_{11} + ... + 2hka^*b^*U_{12})$.

Results and Discussion

Addition of O_2 to $[Cu^I(TMPA)CH_3CN]PF_6$ (**1**) in acetonitrile at room temperature results in a formation of a transient purple solution (indicative of presence of a copper–dioxygen complex[6b]), which then produces a cloudy blue solution. Precipitation with ether and recrystallization of the resulting solid from CH_2Cl_2–Et_2O in general gives rise to a low-yield mixture of both light and dark

$$[Cu^I(TMPA)CH_3CN]PF_6 + O_2 \xrightarrow[\text{2. crystallize: } CH_2Cl_2\text{–}Et_2O]{\text{1. } CH_3CN} \underset{\mathbf{2}}{[Cu^{II}(TMPA)F]_2(PF_6)_2} + \underset{\mathbf{3a};\ S = CH_2Cl_2 \quad \mathbf{3b};\ S = {}^1/_2H_2O}{[Cu^{II}(TMPA)F]PF_6 \cdot S}$$

blue crystalline material.[8] The dark blue crystals have been identified as $[Cu^{II}(TMPA)F]_2(PF_6)_2$ (**2**) based on an X-ray crystallographic analysis as well as other physicochemical data. The light blue product has been formulated as $[Cu^{II}(TMPA)F]PF_6 \cdot CH_2Cl_2$ (**3a**), also on the basis of an X-ray crystal structure.

(8) The light and dark blue crystals in the mixture are separated by hand according to color and crystal morphology. In certain instances, only one type of crystal is observed following recrystallization. Unfortunately, we have not yet been able to determine what conditions favor the crystallization of one compound over the other.

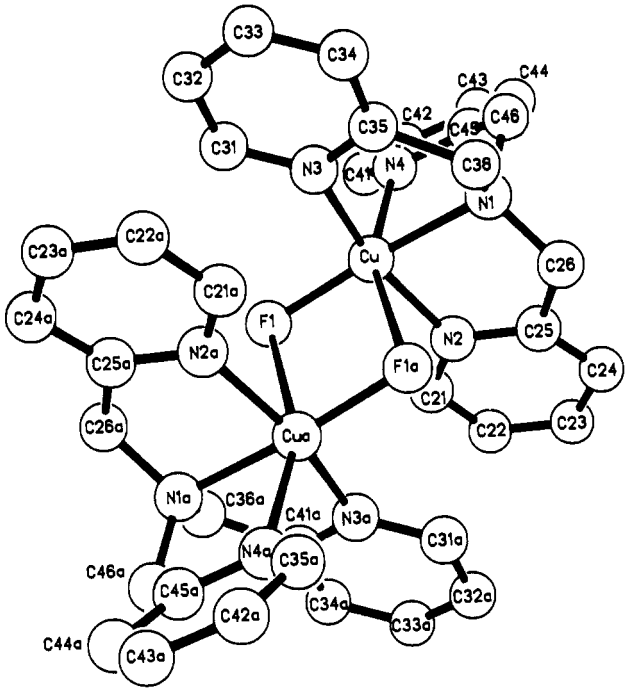

Figure 1. ORTEP diagram of the cationic portion of $[Cu^{II}(TMPA)F]_2(PF_6)_2$ (**2**), showing the atom-labeling scheme.

When allowed to stand in air, **3a** loses its CH_2Cl_2 solvate and absorbs water to form $[Cu^{II}(TMPA)F]PF_6 \cdot {}^1/_2H_2O$ (**3b**). This formulation is confirmed by elemental analysis on **3b** and the solvate-free product $[Cu^{II}(TMPA)F]PF_6$, formed by heating **3b** under a vacuum. A thermogravimetric (TGA) experiment also quantitatively confirmed the half water solvate per copper complex formulation. As is typical in complexes with water, **3b** has multiple IR absorptions between 3650 and 3000 cm^{-1} and at 1655 cm^{-1}. Emsley and co-workers have amply demonstrated the occurrence of hydrogen-bonded water in metal–fluoride complexes,[5c,9] and the presence of a LCu–F···HOH···F–CuL would not only fit the stoichiometry observed here but also be in accord with a crystallographically observed case having a water molecule hydrogen bonded between two Cu–F moieties.[5e]

The source of fluoride ion in these compounds is clearly the PF_6^- anion since the yields (based on copper) are always found to be less than 50% and the corresponding Cu(I) perchlorate complex $[Cu^{I}(TMPA)CH_3CN]ClO_4$ did not react to give any similar fluoride complex under identical conditions. Presumably, decomposition of the PF_6^- anion occurs during reaction of the Cu(I) complex with O_2, releasing the F^- ion, which can then be incorporated into the cupric compounds.[10] Similar fluoride abstraction reactions are well-known to occur in transition-metal complexes containing the tetrafluoroborate anion,[5a-e,11] often resulting in well-defined metal–fluoride coordination compounds. Fluoride abstraction from PF_6^- appears to be very rare, but there is another recent example described for a chromium organometallic complex.[12] The mechanism of metal–fluoride formation involving BF_4^- breakage is apparently unknown, although Reedijk has suggested a possible pathway that involves the attack of a heterocyclic amine ligand upon a coordinated tetrafluoroborate anion.[5a] We made no attempt to initiate mechanistic investigations concerning PF_6^- decomposition in our system.

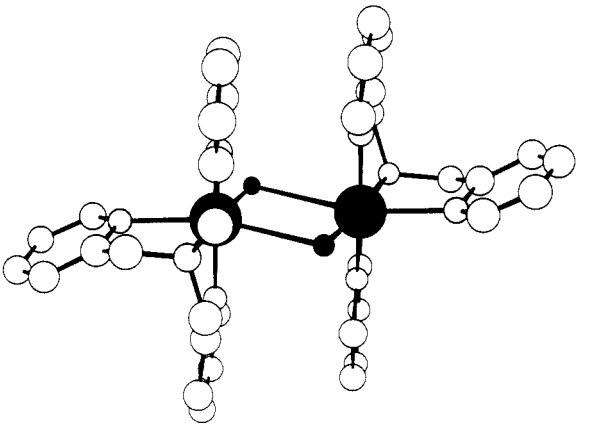

Figure 2. Perspective drawing for the cationic portion of complex $[Cu^{II}(TMPA)F]_2(PF_6)_2$ (**2**), indicating the stacking of pyridine rings of the ligand.

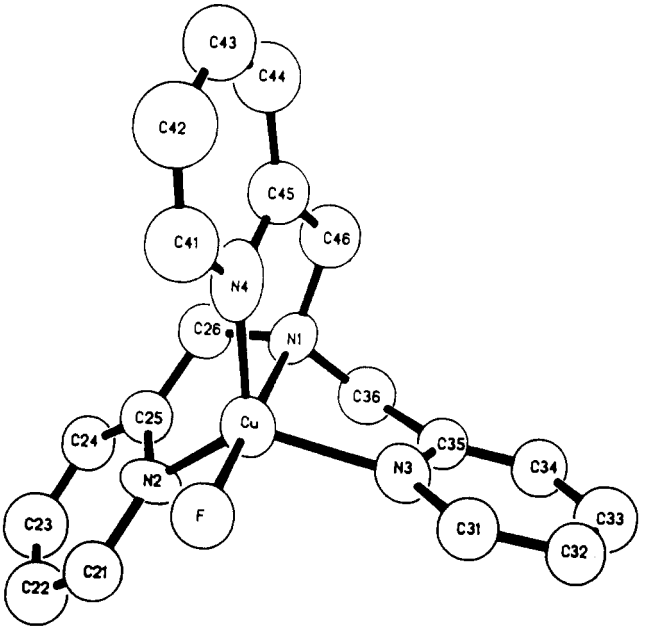

Figure 3. ORTEP drawing of the cationic portion of $[Cu^{II}(TMPA)F]PF_6 \cdot CH_2Cl_2$ (**3a**), showing the atom-labeling scheme.

As shown in Figure 1, the structure of $[Cu^{II}(TMPA)F]_2(PF_6)_2$ (**2**) consists of two monomeric $[Cu^{II}(TMPA)F]^+$ cations bound together by long axial Cu–F interactions to form a weakly linked dimeric unit. The halves of the dimer are related by a crystallographic center of symmetry midway between the two copper(II) ions; the Cu···Cu distance is 3.444 (1) Å (Table IV). The coordination geometry about each copper atom is pseudooctahedral with the axial positions being occupied by a pyridyl nitrogen (N4) and the fluorine atom with the longer Cu–F bond length (2.960 (5) Å). The equatorial plane is composed of a second fluorine atom (Cu–Fl = 1.862 (4) Å), the aliphatic amine nitrogen (N1), and remaining pyridyl donors (N2, N3). As expected, the axial Cu–N4 distance (2.329 (5) Å) is significantly longer than that of the other copper–nitrogen bonds (2.002 Å average). Thus, the overall coordination can be described as "parallel–planar", i.e. with joining of the copper coordination spheres through axial- and basal-edged (equatorial) bridging atoms. This structure closely resembles the parallel–planar structure formed in the dihydroxo-bridged dimer $[Cu^{II}(BPY)OH]_2(PF_6)_2$ (BPY = bis(2-(2-pyridyl)ethyl)benzylamine), where there is one less donor group present per copper ion, since BPY is a tridentate ligand.[13]

(9) (a) Emsley, J.; Arif, M.; Bates, P. A.; Hursthouse, M. B. *J. Chem. Soc., Chem. Commun.* **1989**, 738–739. (b) Emsley, J.; Arif, M.; Bates, P. A.; Hursthouse, M. B. *J. Chem. Soc., Dalton Trans.* **1989**, 1273–1276. (c) Emsley, J.; Arif, M.; Bates, P. A.; Hursthouse, M. B. *J. Chem. Soc., Chem. Commun.* **1988**, 1387–1388. (d) Emsley, J.; Arif, M.; Bates, P. A.; Hursthouse, M. B. *Inorg. Chim. Acta* **1989**, *154*, 17–20.

(10) We have observed the formation of Cu(II)–fluoride complexes in the reactions of O_2 with at least two other copper(I) compounds containing tripod ligands and the PF_6^- anion. In one case X-ray crystallographic characterization showed the resulting fluoride complex to have a dimeric structure similar to that of **2**.[6c]

(11) (a) Gorrell, I. B.; Parkin, G. *Inorg. Chem.* **1990**, *29*, 2452–2456. (b) Reedijk, J.; Jansen, J. C.; van Koningsveld, H.; van Kralingen, C. G. *Inorg. Chem.* **1978**, *17*, 1990–1994.

(12) Thomas, B. J.; Mitchell, J. F.; Theopold, K. H.; Leary, J. A. *J. Organomet. Chem.* **1988**, *348*(3), 333–342.

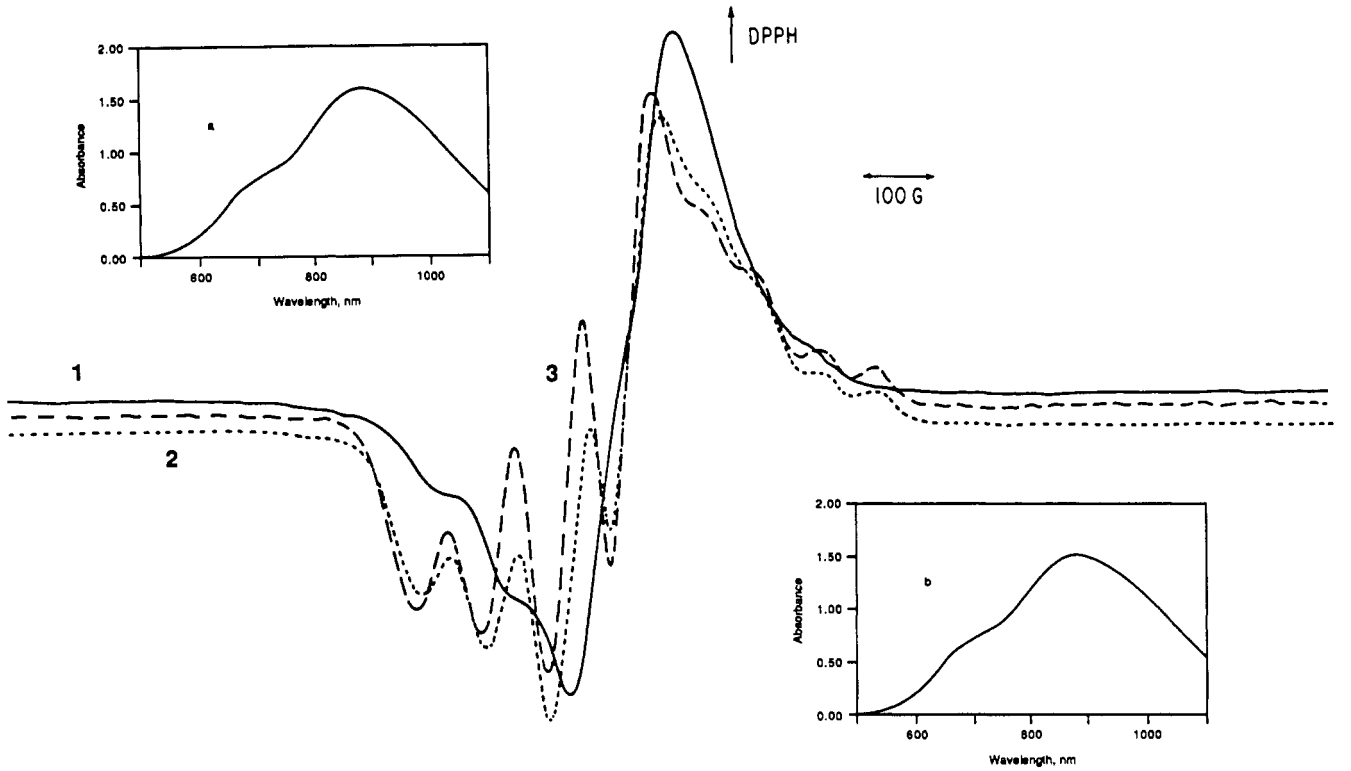

Figure 4. EPR spectra (EtOH–MeOH, 4:1 (v/v) 77 K) of $[Cu^{II}(TMPA)H_2O](ClO_4)_2$ (**4**) (spectrum 1), $[Cu^{II}(TMPA)F]PF_6 \cdot {}^1/_2H_2O$ (**3b**) (spectrum 2), and $[Cu^{II}(TMPA)H_2O](ClO_4)_2$ (**4**) plus 5 equiv of $Bu_4NF \cdot H_2O$ (spectrum 3). The insets show the UV–vis spectra of **3b** (spectrum a) and **4** plus 5 equiv of $Bu_4NF \cdot 3H_2O$ (spectrum b) in the same solvent mixture.

Table IV. Selected Bond Distances (Å) and Angles (deg) for Complexes **2** and **3a**

$[Cu^{II}(TMPA)F]_2(PF_6)_2$ (**2**)		$[Cu^{II}(TMPA)F]PF_6 \cdot CH_2Cl_2$ (**3a**)	
	Interatomic Distances		
Cu–F1	1.862 (4)	Cu–F1	1.853 (8)
Cu–N1	2.040 (5)	Cu–N1	2.069 (10)
Cu–N2	1.985 (5)	Cu–N2	2.014 (9)
Cu–N3	1.981 (5)	Cu–N3	2.044 (8)
Cu–N4	2.329 (5)	Cu–N4	2.013 (10)
Cu–F1a	2.960 (5)		
Cu···Cua	3.444 (1)		
	Interatomic Angles		
F1–Cu–N1	171.8 (2)	F1–Cu–N1	179.5 (4)
F1–Cu–N2	96.8 (2)	F1–Cu–N2	99.0 (3)
N1–Cu–N2	83.7 (2)	N1–Cu–N2	81.5 (4)
F1–Cu–N3	96.2 (2)	F1–Cu–N3	99.3 (3)
N1–Cu–N3	82.1 (2)	N1–Cu–N3	80.5 (3)
N2–Cu–N3	164.1 (2)	N2–Cu–N3	117.7 (3)
F1–Cu–N4	107.6 (2)	F1–Cu–N4	98.1 (3)
N1–Cu–N4	80.6 (2)	N1–Cu–N4	81.5 (3)
N2–Cu–N4	84.6 (2)	N2–Cu–N4	124.8 (4)
N3–Cu–N4	100.0 (2)	N3–Cu–N4	110.6 (3)
Cu1–F1a–Cua	88.0 (2)		
F1–Cu–F1a	92.0 (2)		
N1–Cu–F1a	79.9 (2)		
N2–Cu–F1a	88.7 (2)		
N3–Cu–F1a	81.8 (2)		
N4–Cu–F1a	159.9 (2)		

Stabilization of this dimer structure is apparently aided by a pronounced stacking interaction (Figure 2) of two sets of pyridine rings, i.e. those containing N2 and N3a and those containing N3 and N2a (Figure 1). These rings are staggered but on top of each other with ring–ring distances of ~3.45 Å, close to the value of the Cu···Cu distance. This sort of interaction is also found in $[Cu^{II}(BPY)OH]_2(PF_6)_2$.[13]

(13) Karlin, K. D.; Gultneh, Y.; Hayes, J. C.; Zubieta, J. *Inorg. Chem.* **1984**, *23*, 519–521 and references cited therein.

In contrast to **2**, complex **3a** is strictly monomeric, the closest approach of any two copper atoms being greater than 6.73 Å (Figure 3). Here, the coordination geometry is trigonal bipyramidal (TBP), with the fluorine and aliphatic amine nitrogen atoms occupying axial positions and the equatorial plane composed of the three pyridyl nitrogens. The Cu(II) ion lies 0.305 Å out of the equatorial plane and is displaced away from the aliphatic amine nitrogen as a result of the acute N_{py}–Cu–N_{amine} bond angles (81.2° average) (Table IV). The axial coordination is nearly linear, with a N1–Cu–F bond angle of 179.7 (4)°. The copper–fluorine bond distance in **3a** (1.853 Å) is among the shortest ones known for copper–fluoride complexes.[5e]

Spectroscopic data obtained on **2** and **3b** are also consistent with the X-ray crystallographic characterization. For example, the powder EPR spectrum of **2** shows a well-resolved pattern typical of an isolated Cu_2 dimer with an absorption corresponding to a $\Delta M_s = 2$ transition at $g \approx 4$. Mull transmittance spectra also support an octahedral geometry about Cu(II) in **2** (λ_{max} = 677 nm). While the EPR spectrum of **2** is indicative of the dimer structure, the observed magnetic moment of, $\mu_{eff} = 1.95 \pm 0.05$ μ_B/Cu, suggests the presence of only a negligible or very weak Cu(II)···Cu(II) electronic interaction, undoubtedly due to this axial–equatorial bridging fluoride network. The powder spectrum of **3b** shows no low-field $\Delta M_s = 2$ transition, which is expected on the basis of the known monomeric structure. The solid-state UV–vis spectrum of **3b** is typical for complexes having a trigonal-bipyramidal geometry (λ_{max} = 872 and 710 (sh) nm), as copper(II) complexes in TBP geometry often possess this d–d pattern with a lower energy peak and a higher energy less intense shoulder.[6a,d,14]

(14) (a) Nakao, Y.; Onoda, M.; Sakurai, T.; Nakahara, A.; Kinoshita, I.; Ooi, S. *Inorg. Chim. Acta* **1988**, *151*, 55–59. (b) Addison, A. W.; Hendriks, H. M. J.; Reedijk, J.; Thompson, L. K. *Inorg. Chem.* **1981**, *20*, 103–110. (c) Thompson, L. K.; Ramaswamy, B. S.; Dawe, R. D. *Can. J. Chem.* **1978**, *56*, 1311. (c) Ciampolini, M.; Nardi, N. *Inorg. Chem.* **1966**, *5*, 41. (f) Albertin, G.; Bordignon, E.; Orio, A. A. *Inorg. chem.* **1975**, *14*, 1411. (g) Duggan, M.; Ray, N.; Hathaway, B.; Tomlinson, G.; Briant, P.; Plein, K. *J. Chem. Soc., Dalton Trans.* **1980**, 1342. (h) Hathaway, B. J.; Billing, D. E. *Coord. Chem. Rev.* **1970**, *5*, 143. (i) Hathaway, B. J. *J. Chem. Soc., Dalton Trans.* **1972**, 1196.

Several lines of evidence point to the fact that both **2** and **3b** have a common structure in solution, i.e. **2** apparently dissociates to give a monomeric species that is identical with **3**. Thus, dissolution of **2** and **3b** results in identical UV-vis and "reversed axial" frozen-solution EPR spectra (see Experimental Section). Copper(II) complexes in TBP geometry with tripodal ligands normally display a "reversed axial" pattern in the frozen-solution EPR spectra with $g_{\parallel} < 2.0$.[6d,15] The conclusion is also supported by the measured molar conductivities of **2** and **3b**, which are within the range expected for 1:1 electrolytes.[16]

This mononuclear fluorocopper(II) complex could also be generated by using added fluoride in the form of tetrabutylammonium fluoride (Bu_4NF). For these experiments an aqua complex $[Cu^{II}(TMPA)H_2O](ClO_4)_2$ (**4**) was utilized since the water in **4** can be easily replaced and the perchlorate counteranions present cannot serve as a F^- source. Thus, Bu_4NF was added to complex **4** and the reaction was followed by EPR and UV-vis spectroscopy as illustrated in Figure 4. EPR spectrum 1 corresponds to a solution of the aqua complex, $[Cu^{II}(TMPA)H_2O](ClO_4)_2$ (**4**), in a 4:1 mixture of EtOH-MeOH (77 K). Addition of 5 equiv of $Bu_4NF{\cdot}3H_2O$ to the solution of **4** results in a well-resolved EPR spectral pattern (spectrum 3), essentially identical with that of a solution of **3b** (spectrum 2) under the same conditions. The electronic spectra of **3b** and **4** + $5Bu_4NF{\cdot}3H_2O$ are also identical (insets, Figure 4) and different from that of **4**, strongly suggesting that F^- has displaced the aqua ligand in **4** to give a fluoride complex that has solution properties substantially the same as **3b**.

In summary, fluoride-Cu(II) complexes with the tripodal tetradentate ligand TMPA form when the corresponding $[Cu^{I}(TMPA)CH_3CN]PF_6$ complex is reacted with dioxygen. Interesting mono- and dinuclear structures form, demonstrating the flexibility of the TMPA ligand in forming Cu(II) complexes in several coordination geometries (i.e. trigonal bipyramidal and pseudooctahedral) and demonstrating that F^- may serve either as a terminal or bridging ligand in these systems. Further examination of these and other compounds may assist in further understanding the ligating properties of fluoride ion with copper ion complexes and metalloproteins.

Acknowledgment. We are grateful to the National Institutes of Health (K.D.K.) for support of this research. We also thank Dr. Bruce Johnson, General Electric R & D Center, Schenectady NY, for arranging for the thermogravimetric analyses.

Supplementary Material Available: For $[Cu^{II}(TMPA)F]_2(PF_6)_2$ (**2**) and $[Cu^{II}(TMPA)F]PF_6{\cdot}CH_2Cl_2$ (**3a**), full tables of crystal data, atomic coordinates and isotropic thermal parameters, hydrogen atom parameters, bond distances, bond angles, and anisotropic thermal parameters (9 pages); listings of observed and calculated structure factors (24 pages). Ordering information is given on any current masthead page.

(15) (a) Takahashi, K.; Ogawa, E.; Oishi, N.; Nishida, Y.; Kida, S. *Inorg. Chim. Acta* **1982**, *66*, 97-103. (b) Barbucci, R.; Bencini, A.; Gatteschi, D. *Inorg. Chem.* **1977**, *16*, 2117. (c) Thompson, L. K.; Ramaswamy, B. S.; Dawe, R. D. *Can. J. Chem.* **1978**, *56*, 1311.
(16) Geary, W. J. *Coord. Chem. Rev.* **1971**, *7*, 81-122.

Contribution from the Faculty of Chemistry, University of Bielefeld, D-4800 Bielefeld 1, West Germany

Preparation and X-ray Structure of Tetraphenylphosphonium Amminebis(tetrasulfido)nitrosylruthenate, $(PPh_4)[Ru(NO)(NH_3)(S_4)_2]$: The First Polysulfido Nitrosyl Complex of Ruthenium

A Müller,* M. Ishaque Khan,† E. Krickemeyer, and H. Bögge

Received August 6, 1990

$(PPh_4)[Ru(NO)(NH_3)(S_4)_2]$ has been prepared by reacting trichloronitrosylruthenium with a solution of tetraphenylphosphonium polysulfide in ammoniacal acetonitrile and characterized by X-ray crystallography. Crystal data at 21 °C: dark red-brown crystals, monoclinic space group $P2_1/n$, a = 11.341 (3) Å, b = 13.091 (3) Å, c = 20.829 (5) Å, β = 104.93 (2)°, V = 2987.8 Å^3, Z = 4; the structure was refined to R = 0.046 and R_w = 0.043 for 4986 unique reflections. Ru-N(NO), Ru-N(NH_3), and Ru-S distances are 1.717 (4), 2.146 (4), and 2.394 (1)-2.408 (1) Å, respectively. The Ru-NO moiety is approximately linear, with an Ru-N-O angle of 175.7 (3)°.

Introduction

(Polysulfido)metal complexes are of current interest.[1,2] Studies in this area have been further motivated due to evidence of the significant roles played by metal sulfide species in some vital industrial[3] (e.g. fuel processing/hydrodesulfurization catalysis[1,2]) and biological[4] (e.g. electron transfer and nitrogen fixation) processes.

Consequently, a sizable literature on syntheses, characterization, and reactivities of these complexes, some of which have been characterized by X-ray crystallography, is now available.[1] There appears to be, however, a striking paucity of the similar complexes of ruthenium, and only few polysulfido complexes of the latter have been reported,[5] despite the fact that a number of complexes exist with monodentate and/or polydentate ligands bonded to ruthenium through sulfur.[6]

Our interest in (polysulfido)ruthenium complexes stems mainly from the known special efficacy of ruthenium disulfide as a hydrodesulfurization catalyst[7] (e.g., RuS_2 displays better oxygen chemisorption and catalytic activity toward thiophene hydrodesulfurization than the conventional MoS_2 catalyst).[7b] Additional

† On leave from the Department of Chemistry, Aligarh Muslim University, Aligarh-202002, India.

(1) (a) Müller, A.; Diemann, E. *Adv. Inorg. Chem.* **1987**, *31*, 89. (b) Draganjac, M.; Rauchfuss, T. B. *Angew. Chem.* **1985**, *97*, 745; *Angew. Chem., Int. Ed. Engl.* **1985**, *24*, 742.
(2) Stiefel, E. I.; Chianelli, R. R. In *Nitrogen Fixation: The Chemical-Biochemical-Genetic Interface*; Müller, A., Newton, W. E., Eds.; Plenum Press: New York, 1983; p 341.
(3) (a) Weisser, O.; Landa, S. *Sulphide Catalysts, Their Properties and Applications*; Pergamon Press: Oxford, England, 1973. (b) Rakowski DuBois, M. *Chem. Rev.* **1989**, *89*, 1. (c) Müller, A.; Diemann, E.; Baumann, F.-W. *Nachr. Chem. Tech. Lab.* **1988**, *36*, 18.
(4) Newton, W. E. In *Sulfur: Its Significance for Chemistry, for the Geo-, Bio- and Cosmosphere and Technology*; Müller, A., Krebs, B., Eds.; Elsevier: Amsterdam, 1984; p 409.
(5) (a) Gotzig, J.; Rheingold, A. L.; Werner, H. *Angew. Chem.* **1984**, *96*, 813; *Angew. Chem., Int. Ed. Engl.* **1984**, *23*, 814. (b) Amarasekera, J.; Rauchfuss, T. B.; Rheingold, A. L. *Inorg. Chem.* **1987**, *26*, 2017. Ogilvy, A. E.; Rauchfuss, T. B. *Organometallics* **1988**, *7*, 1884. (c) Brunner, H.; Janietz, N.; Wachter, J.; Nuber, B.; Ziegler, M. L. *J. Organomet. Chem.* **1988**, *356*, 85. (d) Wachter, J. *Angew. Chem.* **1989**, *101*, 1645; *Angew. Chem., Int. Ed. Engl.* **1989**, *28*, 1613.
(6) Schröder, M.; Stephenson, T. A. In *Comprehensive Coordination Chemistry*; Wilkinson, G., Gillard, R. D., McCleverty, J. A., Eds.; Pergamon Press: Oxford, England, 1987; Vol. 4, Chapter 45.

0020-1669/91/1330-2040$02.50/0